

Estimations of the effects of the middle atmosphere on the transmission of a high-power laser beam.

Part 1. The atmospheric model, the influence of nonlinear effects on the transmission of the Gaussian and super-Gaussian laser beams

V.V. Vorob'ev, V.M. Osipov, and Ya.A. Rezunkov

*Research Institute for Complex Testing of Optoelectronic Devices and Systems,
Sosnovy Bor, Leningrad Region*

Received November 26, 2002

On the basis of analytical overview of the present-day models of aerosol and gas components of the atmosphere, the model has been developed to calculate the laser radiation transmission at altitudes higher than 10 km, and the coefficients of extinction, absorption, and scattering of laser radiation are determined for the cases of vertical and slant atmospheric paths. The conditions are formulated for the parameters of Gaussian and super-Gaussian beams when the distortions due to the nonlinear effects of the interaction of a laser pulse with the upper atmosphere can be neglected.

Introduction

At present several projects exist aimed at the use of laser jet thrust both for launching space vehicles to orbit¹ and for the transfer of space vehicles from the low near-Earth orbits to a geostationary orbit² with the use of high-power pulse-periodic lasers. The idea of using high-power lasers for these purposes takes its name in the English literature as LOTV (Laser Orbital Transfer Vehicle).² The mass of a space vehicle along with the mass of the rocket propellant for a laser jet engine can reach several tons (up to 10 tons). Theoretical estimations³ show that the necessary jet thrust at the level of 100 to 200 N for such orbital flights can be maintained by the pulse-periodic lasers at the radiation power of 500 kW. In this case the jet thrust is much less than the attractive force of the heavy space vehicle by the Earth, and the regime of the vehicle change-over corresponds to the regime of low thrust. In the regime of low jet thrust the space vehicle will be transported from one orbit to another on a spiral path.

It is also assumed that it is the best to locate a laser higher than the denser layers of the atmosphere (the position of the laser is on the mountain or onboard an aircraft to reduce the influence of the atmosphere on the efficiency of power transportation to the space vehicle. Therefore during an active contact of the aircraft with the space vehicle one can consider to sufficient accuracy its orbit to be a circle. In this case the path length of laser beam propagation in the atmosphere can be given by such parameters as the radii of orbits of an aircraft flight and a satellite flight and zenith angle of the laser beam propagation direction.

References 1–3 describe serially the influence of nonlinear effects and turbulence on the laser radiation

transmission through the atmosphere. Efficiency of the laser beam power delivery is also determined by the size of the aperture of receiving and transmitting telescopes, both airborne and spaceborne. The use of an airborne laser imposes restriction on the aperture of the transmitting telescope. Most likely the mirror diameter of the transmitting telescope is equal to 1.0–1.5 m. At the same time, within the context of the concept of LOTV the diameter of the receiving collector of laser radiation for various reasons is limited. In the literature² the aperture of the receiving mirror of the collector is chosen to be equal to 4.5 m. In this case at orbits located higher than 1000 km the receiving mirror diameter of LOTV vehicle will be smaller than the diffraction size of a laser beam. Therefore taking into account the effect of the atmosphere on the laser beam transmission in this case becomes especially important because the decrease of the laser beam power, received by the vehicle at high orbits, can result in a considerable decrease of the value of the laser jet thrust, and, hence, in a significant delay of transfer of the vehicle to a geostationary orbit.

It can also be assumed that the most promising types of lasers for realization of this concept are Nd:YLF lasers with diode pumping as well as Nd-lasers activated by Yb ions. Such lasers have been functioning at the wavelengths of 1.053 μm and 1.029 μm (the second harmonic is 0.5265 μm and 0.5145 μm , respectively). Because the experimental data on the laser beam transmission with the above-mentioned parameters for the paths, being of interest for us, are not available in the literature, in this paper, based on the unified model of aerosol and gas atmospheric components at altitude higher than 10 km, the analytical and numerical estimations of the radiation absorption by the atmosphere are made. The paper also describes the influence of such

nonlinear atmospheric effects as thermoblooming, electrostriction, and the Kerr effect on the laser beam transmission as applied to the LOTV conception.

1. Attenuation of laser radiation by atmospheric molecular and aerosol components

Laser radiation at the above indicated wavelengths is only slightly attenuated by the atmosphere. However, when transmitting high-power radiation through the atmosphere, such nonlinear effects as thermal beam defocusing and the optical breakdown of atmospheric gases can have great impact on the laser beam characteristics. Threshold values and the degree of these effects influence are determined by optical, thermodynamic, and microphysical characteristics of aerosol and gas atmospheric components. Therefore, the choice of atmospheric models for altitudes above 10 km, containing the required information about the optical characteristics both of aerosol and gas components of the atmosphere, is very important for evaluating these effects.

By now, in Russia and abroad a great number of different models of the aerosol atmosphere have been developed.⁴ On the basis of specific properties of this problem, the principal criterion for selecting an appropriate model is the degree of statistical significance of the determination of its characteristics in the atmospheric layer above 10 km. During the past ten years wide-range investigations of stratospheric aerosol characteristics have been performed using the SAM-2, SAGE-I, and SAGE-II⁵ instrumentation. These experiments make it possible to obtain vertical profiles of the aerosol extinction coefficient at four wavelengths (0.385, 0.453, 0.525, and 1.02 μm) in the $\pm 80^\circ$ latitude range for the upper troposphere and stratosphere. The obtained information was used for creation and systematic correction of the aerosol atmosphere model, being used as a part first in the procedure of atmospheric transmission calculation with low spectral resolution (Lowtran procedure⁶) and then being a component of most of other engineering and computer methods of the calculation of atmospheric transmission (Fascod, Modtran and others). Based on a comparison of different aerosol models with the latest experimental measurements (see, in particular, the results in Ref. 7), one can draw a conclusion that of all the models of optical characteristics of aerosol in the middle atmosphere, the Lowtran model⁶ most closely agrees with the present-day experimental data.

At present, in solving research and applied problems several models of composition and parameters of gaseous atmosphere are used. They represent the averaged experimental data on high-altitude distribution of the temperature, pressure, and density of the air as well as high-altitude concentration of individual molecular components. In Russia, as a rule, three models: the model of State Optical Institute, the model of the IAO SB RAS,⁸ the model of AFGL⁹

are used. The model of AFGL is the best known in the world scientific literature and a basic one in solving the problems of radiation transfer in the atmosphere. As a model of aerosols in the Lowtran methods, this model is corrected in regular intervals while taking into account the latest experimental data. In view of this situation it is the model of AFGL that has been used in this paper. Numerical values of high-altitude profiles are set according to recent version of this model published in Ref. 10.

Using the above-mentioned models of aerosol and gaseous atmosphere we have determined the extinction and absorption coefficients of the atmosphere necessary in evaluating linear and nonlinear processes at laser radiation transmission along atmospheric paths being of interest for us.

Recall that the expression for monochromatic absorption $A_{Z_0}(\lambda)$ for the vertical path coming from the height Z_0 to the atmospheric top Z_{atm} can be written in the following form:

$$A_{Z_0}(\lambda) = \int_{-\infty}^{\infty} \{1 - \exp[-D_{Z_0}(\lambda')]\} d\lambda', \quad (1)$$

where $D_{Z_0}(\lambda)$ is the optical thickness of the atmospheric path ($D_{Z_0} = \int_{Z_0}^{Z_{\text{atm}}} K(\lambda, z) dz$), and the

extinction coefficient K in the linear approximation includes the absorption coefficient K_a and the scattering coefficient K_{sc} that, in turn, are determined by sum of these quantities for gaseous K^{m} and aerosol K^{a} components of the atmosphere, i.e.,

$$K = K_a + K_{\text{sc}} = K_a^{\text{m}} + K_a^{\text{a}} + K_{\text{sc}}^{\text{m}} + K_{\text{sc}}^{\text{a}}. \quad (2)$$

As was mentioned above, we use in this paper, the Lowtran model to calculate the values of aerosol absorption K_a^{a} and scattering K_{sc}^{a} . The molecular scattering coefficient K_{sc}^{m} can easily be calculated. The central problem is to determine the value of molecular absorption. The complex structure of molecular absorption spectra in the range of 0.5–1.2 μm , caused by the presence of both the diffuse and structured absorption bands, results in the necessity of using a combined methods of the calculation containing the approximate expressions for calculating the continuous absorption and precise line-by-line methods to calculate the transmission in structured absorption bands.¹¹ To make such calculations, it is necessary to use three databases:

- the database on the composition and parameters of gas and aerosol atmosphere for different seasons and geographic regions (above-mentioned atmospheric models);
- the database on parameters of spectral lines of separate gas components with the resolved rotational structure;
- the database on the absorption cross section of gas components with unresolved rotational structure.

Bank of spectroscopic parameters of spectral lines of atmospheric gases was formed on the basis of recent versions of the known data bank HITRAN.¹²

Data bank on the absorption cross sections of gas components with unresolved rotational structure is necessary in this paper for calculating the absorption in the range of 0.5 μm, i.e., at frequencies of second harmonic generation of the earlier mentioned lasers. In this paper for solving this problem we used the first version of data bank created in Ref. 11 on the absorption cross section of basic and contaminating components of the atmosphere as well as products of combustion of rocket and aircraft engines (bank UVACS).

Calculations of the absorption coefficients of aerosol K^a and molecular K^m atmospheric components as well as the net absorption coefficient K_a were performed with the use of an algorithm described in detail in Ref. 13. Figure 1 shows the calculated results on the net absorption coefficient for laser radiation at $\lambda_1 = 0.5265 \mu\text{m}$ and $\lambda_2 = 1.053 \mu\text{m}$ (second harmonic and the fundamental frequency of Nd:YLF laser) depending on altitude.

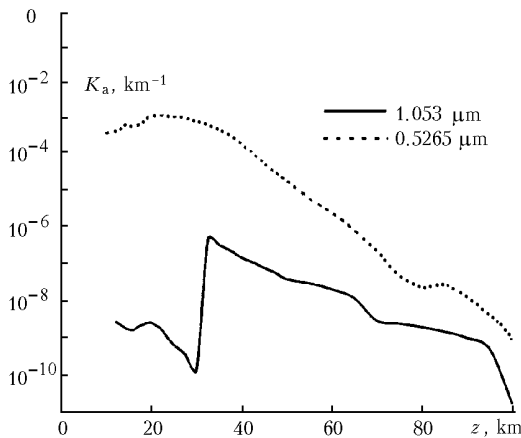


Fig. 1. Height profile of the total absorption coefficient at the two wavelengths for spring and summer.

Near 1 μm the coefficient of molecular absorption, determined in this spectral range by the wings of rare lines of water vapor absorption, is very small, and the net molecular extinction coefficient is usually equal to the molecular (Rayleigh) scattering coefficient. Really the generation line at $\lambda = 1.053 \mu\text{m}$ falls between the absorption lines, however, a small shift of generation frequency can change the value of molecular absorption by several orders of magnitude. Nevertheless, even in this case the molecular absorption along the vertical path will be no more than several thousandths of percent.

Quite different situation occurs in the range of this frequency harmonic, at the wavelength of $\lambda_1 = 0.5265 \mu\text{m}$. Here the molecular absorption is determined by the atmospheric ozone, whose spectrum in this spectral range has a smooth structure, and the maximum of volume concentration is located at 35 km altitude. Because of a great value of the molecular

absorption coefficient the total absorption coefficient at the wavelength of 0.5265 μm is much greater than at $\lambda = 1.053 \mu\text{m}$.

As the assessments show for Nd-laser, doped with Ytterbium (Yb) ions, the altitude dependence of the total absorption coefficient for the fundamental frequency and its second harmonic is of the same character and being only a little smaller in magnitude.

2. The effect of thermal nonlinearity on the laser beam propagation

The values of the aerosol and molecular absorption coefficients obtained previously were used to assess the variations of the laser beam parameters due to thermal blooming in the atmosphere. The effect of thermal nonlinearity on the laser beam propagation was described in the extensive literature. The detailed bibliography was given, for example, in the monographs 14–20. A peculiarity of the above-mentioned problem is that the laser beam, as a whole, can travel across the atmosphere at a speed, compared with the speed of sound. Because the effects of thermal nonlinearity are weak, for evaluating them one can use the phase screen approximation.

The nonlinear phase shift $\varphi_{\text{non}}(x, y)$ at the output of the atmosphere owing to the air heating by a laser beam, moving in parallel to the axis x at the speed V relative to the stationary air, can be calculated by the formula:

$$\varphi_{\text{non}}(x, y) = k \frac{\partial n}{\partial \rho} \int_0^{\xi_{\text{atm}}} \Delta \rho(x, y, \xi) d\xi, \quad (3)$$

where k is the wave number, the coordinate ξ is directed along the axis of beam propagation, θ is the zenith angle, x, y are the transverse coordinates, $\xi_{\text{atm}} = (Z_{\text{atm}} - Z_0) / \cos(\theta)$ is the length of the atmospheric path, Z_{atm} is the height of the conventional upper limit of the atmosphere, above which the atmospheric effect can be neglected, Z_0 is the height of the emitter, and $\Delta \rho$ is the air density perturbation, which at the speed V , less than the speed of sound c_s , can be presented by two components¹⁸:

$$\Delta \rho(x, y, \xi) = \rho_1(x, y, \xi) + \rho_2(x, y, \xi),$$

where

$$\begin{aligned} \rho_1(\xi) &= A(\xi) \int_{-\infty}^x \langle I(x', y, \xi) \rangle dx', \\ \rho_2(\xi) &= B(\xi) \int_{-\infty}^{\infty} dp \int_0^{\infty} [\tilde{I}(x + x', p, \xi) - \tilde{I}(x - x', p, \xi)] \times \\ &\quad \times \exp\left(ipy - \frac{|p|x'}{\sqrt{1-M^2}}\right) dx', \\ \tilde{I}(x, p, \xi) &= \frac{1}{2\pi} \int_{-\infty}^{\infty} \langle I(x, y, \xi) \rangle \exp(-ipy) dy; \end{aligned} \quad (4)$$

$$A(\xi) = \frac{K_a(\xi)}{VC_p T(\xi)}, \quad B(\xi) = \frac{A(\xi)M^2}{2(1-M^2)}.$$

Here K_a is the absorption coefficient, C_p is the air specific heat at constant pressure, T is the unperturbed air temperature, $M = V/c_s$.

Under the action of the beam with the Gaussian distribution of the intensity

$$I(x, y, \xi) = I_0 \exp[-(x^2 + y^2)/a^2],$$

where a is the beam radius at the e^{-1} level

$$\rho_2(x, y, \xi) = -\frac{aB(\xi)}{\sqrt{\pi}} I_0 \int_0^\infty \int_0^\infty \sinh\left(\frac{2x\xi'}{a^2}\right) \cos(py) \times \\ \times \exp\left(-\frac{x^2 + \xi'^2}{a^2} - \frac{p^2 a^2}{4} \frac{|p| |\xi'|}{\sqrt{1-M^2}}\right) d\xi' dp. \quad (5)$$

At the beam axis ($x = 0, y = 0$) the function ρ_2 and its partial derivatives $\partial\rho_2/\partial y$, $\partial^2\rho_2/\partial x^2$, $\partial^2\rho_2/\partial y^2$, $\partial^2\rho_2/\partial x\partial y$ equal zero, therefore, accurate to the terms with third power of transverse coordinates the function ρ_2 can be presented in the form

$$\rho_2(x, y, \xi) = -\frac{1}{2} A(\xi) \frac{I_0(\xi)}{a} g(M) \frac{x}{a}, \\ g(M) = \frac{4}{\sqrt{\pi}} \frac{M^2}{1-M^2} \times \\ \times \int_0^\infty \int_0^\infty x \exp\left[-x^2 - \frac{p^2}{4} - \frac{|p| |x|}{\sqrt{1-M^2}}\right] dx dp. \quad (6)$$

Values of the function $g(M)$ are given in Table 1.

Table 1

M	0	0.1	0.2	0.3	0.4
$g(M)$	0	0.010	0.041	0.097	0.182
M	0.5	0.6	0.7	0.8	0.9
$g(M)$	0.309	0.500	0.800	1.333	2.588

With the same accuracy the function ρ_1 is presented in the form:

$$\rho_1(x, y, \xi) = -\frac{1}{2} \frac{K_a(\xi)a}{VC_p T(\xi)} I_0(\xi) \left[\sqrt{\pi} \left(1 - \frac{y^2}{a^2}\right) + 2 \frac{x}{a} \right],$$

and the sum perturbation in the form:

$$[\rho_1(x, y, \xi) + \rho_2(x, y, \xi)]_{x,y \rightarrow 0} = \\ = -\frac{1}{2\pi} \frac{K_a(\xi)}{VC_p T(\xi)} \frac{P(\xi)}{a} \left[\sqrt{\pi} \left(1 - \frac{y^2}{a^2}\right) + [2 + g(M)] \frac{x}{a} \right], \quad (7)$$

where $P(\xi) = \pi a^2 I_0(\xi)$ is the laser radiation power.

The phase shift caused by the thermal blooming φ_{non} in the near axis beam region ($x \ll a, y \ll a$) is given in the form:

$$\varphi_{\text{non}}(x, y) = k [S_0 - \beta_x x + (y^2/2F_y)], \quad (8)$$

where S_0 is the constant, and the quantities characterizing the tilt of the wave front β_x and the radius of its curvature F_y , with the account of the ratios (7) and (8), are given by the following formulas:

$$\beta_x = \frac{1}{VC_p T} \frac{P_0}{\pi a^2} \frac{\partial n}{\partial \rho} \left(1 + \frac{g(M)}{2}\right) \frac{D_{\text{abs}}}{\cos(\theta)}; \quad (9)$$

$$F_y = \left[\frac{\sqrt{\pi}}{VC_p T} \frac{P_0}{\pi a^3} \frac{\partial n}{\partial \rho} \frac{D_{\text{abs}}}{\cos(\theta)} \right]^{-1}. \quad (10)$$

The value of D_{abs} in Eqs. (9) and (10) is the part of the optical thickness of the vertical path

determined by the integral $D_{\text{abs}} = \int_{Z_0}^{Z_{\text{atm}}} K_a(z) dz$, where

K_a is the total coefficient of the aerosol and molecular absorption. Values of D_{abs} for two values of the altitude of location of a laser source (aircraft) Z_0 and at $Z_{\text{atm}} = 100$ km calculated by the above methods, are presented in Table 2.

Table 2

Path parameter	Winter	Summer
$D_{\text{abs}} (\lambda_1 = 0.514 \mu\text{m}, Z_0 = 10 \text{ km})$	0.0153	0.0133
$D_{\text{abs}} (\lambda_1 = 0.514 \mu\text{m}, Z_0 = 15 \text{ km})$	0.0127	0.0119
$D_{\text{abs}} (\lambda_2 = 1.029 \mu\text{m}, Z_0 = 10 \text{ km})$	$2.86 \cdot 10^{-5}$	$3.98 \cdot 10^{-5}$
$D_{\text{abs}} (\lambda_2 = 1.029 \mu\text{m}, Z_0 = 15 \text{ km})$	$3.77 \cdot 10^{-6}$	$3.77 \cdot 10^{-6}$

Instead of the quantity F_y (Eq. (10)) it is convenient to insert the angle of the beam nonlinear divergence $\beta_{\text{non},y}$ in the plane (z, y) as the ratio

$$\beta_{\text{non},y} = \frac{a}{F_y} = \frac{\sqrt{\pi}}{VC_p T} \frac{P_0}{\pi a^2} \frac{\partial n}{\partial \rho} \frac{D_{\text{abs}}}{\cos(\theta)}. \quad (11)$$

Comparing Eqs. (11) and (9) it is seen that the value of the angle of the beam nonlinear divergence coincides accurate to the multiplier $\sqrt{\pi}/[1 + g(M)/2]$ with the value of the angle of wave front tilt of the laser beam.

The relative influence of thermal defocusing can be defined by the ratio of the angle $\beta_{\text{non},y}$ to the angle of diffraction divergence $\beta_d = \lambda/a$, i.e.,

$$Q(\lambda, P, \theta) = \frac{\beta_{\text{non},y}}{\beta_d} = \frac{\sqrt{\pi}}{VC_p T} \frac{P_0}{\pi a \lambda} \frac{\partial n}{\partial \rho} \frac{D_{\text{abs}}(\lambda, Z_0)}{\cos(\theta)}.$$

At the values of the parameters: $a = 0.75$ m, $C_p = 10^3$ J/(kg · deg), $T = 293$ K, $\frac{\partial n}{\partial \rho} = 2.3 \cdot 10^{-4}$ m³/kg,

$V = 100$ m/s, and values $D_{\text{abs}} = 0.015$, $D_{\text{abs}} = 4 \cdot 10^{-5}$ (maxima from Table 2 at the wavelengths $\lambda_1 = 0.514 \mu\text{m}$ and $\lambda_2 = 1.029 \mu\text{m}$) the ratios of angles of nonlinear and diffraction divergences can be written in the form

$$Q(\lambda_1, P, \theta) = 1.73 \cdot 10^{-7} P(W)/\cos(\theta), \quad (12)$$

$$Q(\lambda_2, P, \theta) = 2.29 \cdot 10^{-10} P(W)/\cos(\theta). \quad (13)$$

In Eqs. (12) and (13) the quantity P is the mean radiation power in the sequence of pulses, whose duration is assumed to be longer than the time $t_v = a/V \approx 5$ ms. As follows from Eq. (12), even at the wavelength λ_1 , at which the absorption was maximum, the effect of thermal nonlinearity is insignificant at mean radiation power in a beam less than 1 MW.

The above-mentioned assessments indicate that one can neglect the effect of thermal nonlinearity of the atmosphere on the beam propagation for the considered problem of laser radiation power transfer to the LOTV apparatus. As analogous assessments have shown, the influence of the variation of the refractive index of the atmosphere because of the electrostriction effect can also be neglected.

3. The nonlinearity effect due to the Kerr effect

In contrast to thermal nonlinearity and nonlinearity due to electrostriction, the Kerr effect is a low-inertia one. Typical relaxation times are about 10^{-11} s (Refs. 21, 22). In the steady state the variation of the refractive index is described by the ratio $\Delta n = n_2 |E|^2$, where E is the complex amplitude of the electric field, and n_2 is the constant. It is proportional to the air density. In the literature different data for this quantity are given. According to measurements²¹ it is about $6 \cdot 10^{-17}$ CGSE units for nitrogen at standard atmospheric pressure. The measurements made directly in the air^{19,23} give the value $2.5 \cdot 10^{-16}$ CGSE units. In estimating the magnitude of the effect, the mean altitude distribution of n_2 is considered to be exponential, namely:

$$n_2(z) = n_2(Z_0) \exp[-(z - Z_0)/H_0] \quad (14)$$

with the values of $n_2(Z_0 = 10 \text{ km}) = 3 \cdot 10^{-17}$ CGSE units and $H_0 = 6.5$ km. In a similar way as in determining the effect of thermal nonlinearity, we determine the nonlinear phase shift at the exit from the atmosphere:

$$\varphi_{\text{non}}(x, y) = k \int_0^{\xi_{\text{atm}}} |E(x, y, \xi)|^2 n_2(\xi) d\xi.$$

In the case of the Gaussian beam

$$\varphi_{\text{non}}(x, y) = \varphi_{\text{non}}(0) \exp[-(x^2 + y^2)/a^2],$$

where

$$\varphi_{\text{non}}(0) = kn_2(Z_0) \frac{8P_0 H_0}{ca^2 \cos(\theta)}; \quad (15)$$

P_0 is the laser power, c is the speed of light in vacuum.

The curvature radius corresponding to this phase shift equals:

$$F_{\text{non}} = ka^2 / (2\varphi_{\text{non}}) = \frac{ca^4 \cos(\theta)}{16n_2(Z_0)P_0H_0}.$$

For the beam of radius 0.75 m, generated by a laser, located at 10 km altitude,

$$F_{\text{non}} = 3.04 \cdot 10^{15} \frac{\cos(\theta)}{P_0} \quad (16)$$

(F_{non} is in km, P_0 is in W).

Taking into account the fact that the diffraction lengths $L_d (L_d = ka^2)$ equal to 6680 km at $\lambda = 0.53 \mu\text{m}$ and 3340 km at $\lambda = 1.06 \mu\text{m}$, respectively, it is evident from a comparison of these lengths with the values of F_{non} that the account of the Kerr nonlinearity is necessary if the pulse radiation power is about 10^{12} W. An increase in the altitude of the laser source carrier results in the exponential increase of the value F_{non} and an increase in the values of powers at which the Kerr effect manifests itself.

In connection with the importance of the Kerr effect influence on the laser beam propagation through the atmosphere, its influence was studied using more correct calculation methods. In this case we considered an important for practical applications case of propagation of Gaussian and super-Gaussian beams with the initial distribution of electric field in a beam being as follows:

$$E(x, y, 0) = A_0 \exp\left[-\frac{1}{2} \left(\frac{x^2 + y^2}{a^2}\right)^{N_s}\right]. \quad (17)$$

In particular case when $N_s = 1$, this distribution is Gaussian, and it is super-Gaussian in other cases.

The electric field amplitude A_0 and the radiation power P_0 are connected by the ratio

$$A_0^2 = \frac{8P_0}{ca^2} \frac{N_s}{\Gamma(1/N_s)},$$

where Γ is the gamma function.

To describe the beam propagation, an equation was used for the field intensity of the light wave written in the form:

$$2i \frac{\partial E}{\partial z} + \frac{1}{Ld} \left(\frac{\partial^2 E}{\partial x^2} + \frac{\partial^2 E}{\partial y^2} \right) + 2\varphi_{\text{non}}(0) \frac{N_s}{\Gamma(1/N_s)} f(\xi) |E|^2 E = 0, \quad (18)$$

where the coordinates x and y are normalized to the beam radius a , the quantity $\varphi_{\text{non}}(0)$ is determined by formula (14), and the function $f(\xi)$ at the exponential dependence of $n_2(z)$ equals

$$f(\xi, \theta) = (\cos(\theta)/H_0) \exp(-\xi \cos(\theta)/H_0).$$

In investigating the beam thermal blooming with the initial distributions of the Gaussian type, in which there are no sharp variations of intensity over the aperture and along the propagation axis, the method of phase screens was widely used. However, at the initial distributions with a gap or at sharp variations of the initial intensity on the beam aperture, the intensity distribution in the near field can undergo high-speed oscillations. For providing high precision of calculations in this case, good use can be made of the method of higher order of precision suggested in Ref. 24 in place of the phase screen method.

Figure 2 shows the calculated results on transformation of the intensity distribution of super-Gaussian beams with $N_s = 100$ generated by the laser located at 10 km altitude when the beam propagated along the vertical path ($\theta = 0$). As is seen from the figure, the effect of self-focusing becomes appreciable in the super-Gaussian beam at the pulse power about $0.2 \cdot 10^{12}$ W, and the power about $2 \cdot 10^{12}$ is close to the power, at which the beam portion collapse to a point is possible. These values are approximately five times smaller than the appropriate values of the power for a manifestation of the Kerr nonlinear effect in Gaussian beams. The obtained result is not unexpected. The distance, at which the self-focusing can be realized, depends on the characteristic transverse scales of the radiation intensity. In the super-Gaussian beams these scales in the near zone, in which it is important to take into account the radiation effect on the medium, can be much smaller than in Gaussian beams.

Conclusion

The most promising types of lasers used for realizing the LOTV concept are Nd:YLF lasers with the diode pumping as well as Nd-lasers doped with Yb ions. At their fundamental wavelengths of generation, 1.053 μm and 1.029 μm , and at their second harmonics

the molecular and aerosol radiation extinction and absorption in the upper atmosphere is insignificant (the total extinction for a vertical path at 10 km altitude does not exceed 6%). At mean radiation power (smaller than 1 MW) the beam distortions due to disturbances of the atmospheric refractive index arising because of its heating by the radiation at its absorption are negligible. Nonlinear effects, due to the effect of electrostriction, are also negligible.

The basic nonlinear mechanism, which may have an effect on the laser pulse propagation at peak power about 10^{11} – 10^{12} W, is the Kerr effect. This affects the process of propagation in the case when the nonlinear phase shift ϕ_{non} equals $\pi/2$ in the Gaussian beam and about $\pi/10$ in the beam with super-Gaussian intensity distribution (close to the homogeneous distribution on the round aperture). At the radiation wavelength 1.06 μm , the beam radius of 0.5 m, and vertical propagation, such values of phase shifts are available at powers in the beam being equal to 10^{12} W in the Gaussian beam and $2 \cdot 10^{11}$ W in the super-Gaussian beam. At the wavelength of 0.53 μm the values of the corresponding powers are two times smaller. At the beam power, which is approximately equal to 10^{13} W in Gaussian beams and $2 \cdot 10^{12}$ W in super-Gaussian beams the collapse of the near-axis part of the beam (filamentation) occurs up to dimensions several tens times smaller than the initial beam size.

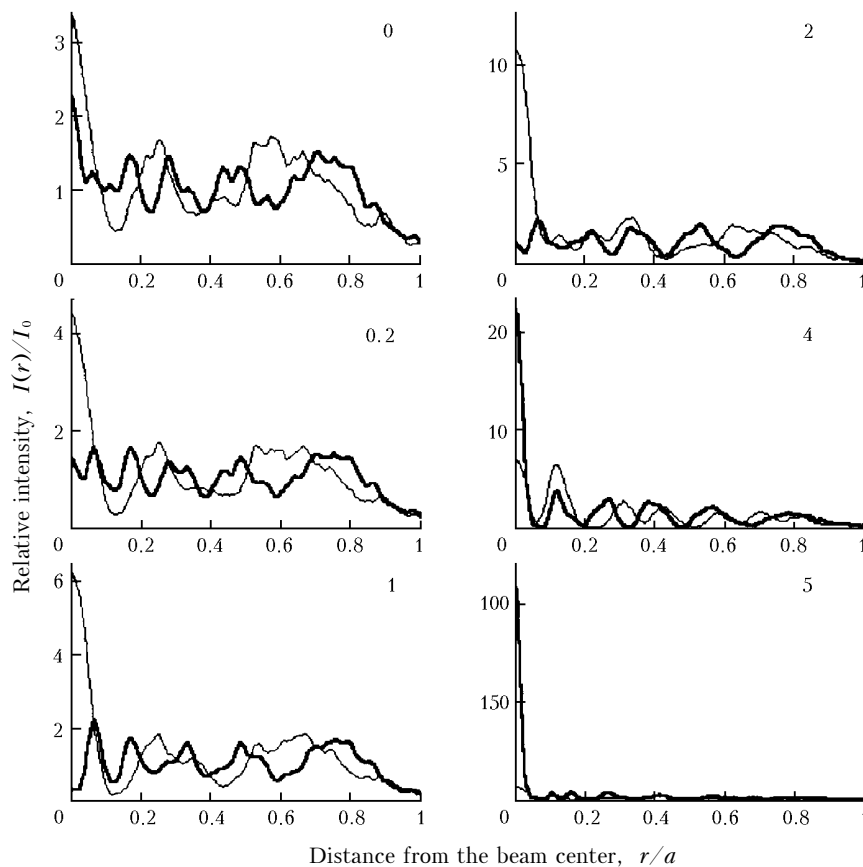


Fig. 2. Intensity distributions at the altitudes of 35 (bold lines) and 60 km (thin lines) in the case of super-Gaussian beams ($N_s = 100$) at $\lambda = 1.06 \mu\text{m}$. The beam power values are in TW.

In this case the model of thermal blooming of radiation calls for further correction that would account for mechanisms preventing the collapse. Among the above-mentioned mechanisms the vector character of thermal blooming in the region of collapse,²⁵ time dispersion,²⁶ and air ionization^{23,24–29} are possible.

Acknowledgments

This work has been performed within the framework of the project ISTC No. 1801).

References

1. L.M. Myrabo, D.G. Messitt, and F.B. Mead, Jr., AIAA Paper, No. 98–1001, 1–10 (1998).
2. Y. Tsujikawa, K. Imasaki, M. Hiino, et al., Proc. SPIE **3885**, *High Power Laser Ablation II*, 54–64 (2000).
3. Yu.A. Rezunkov, A.A. Ageichik, Yu.P. Golovachev, Yu.A. Kurakin, V.V. Stepanov, and A.A. Schmidh, The Review of Laser Engineering **29**, No. 4, 269–273 (2001).
4. G.M. Krekov and R.F. Rakhimov, *Optical Models of Atmospheric Aerosol* (Tomsk Branch SB Acad. Sci. USSR Publisher, Tomsk, 1986), 294 pp.
5. G.K. Ye, M.P. McCormic, W.P. Chu, P. Wang, and M.T. Osborn, J. Geophys. Res. D **94**, No. 5, 8412–8424 (1989).
6. J. E.A. Selby and R.A. McClatchey, *Atmospheric Transmittance from 0.25 to 28.5 μm : Computer Code Lowtran-2*, AFCRL-TR-J2-0745, ADA763721 (1972); Kneizys F.X., G.P. Anderson, E.P. Shettle, et al., *Computer Code LOWTRAN-7*, Air Force Geophysics Laboratory (AFGL), Hanscom, Massachusetts, Environmental research papers, No. 1010 (1988), 235 pp.
7. A.V. Polyakov, Yu.M. Timofeev, A.V. Poberovskii, et al., Izv. Ros. Akad. Nauk, Ser. Fiz. Atmos. Okeana **35**, No. 3, 312–321 (1999).
8. V.E. Zuev and V.S. Komarov, *Statistical Models of the Temperature and Gas Components of the Atmosphere* (Gidrometeoizdat, Leningrad, 1986), 264 pp.
9. R.A. McClatchey, R.W. Tenn, and J.E.A. Selby, *Optical Properties of the Atmosphere*, AFGL-70-0527, No. 331; G.P. Anderson, S.A. Clough, F.X. Kneizys, et al., *AFGL Atmospheric Constituent Profiles (0–120 km)*, Environ. Res. Pap., No. 954, AFGL-TR-86-0110, ADA175173, (1986), p. 44.
10. F.X. Kneizys, L.W. Abreu, and G.P. Anderson, *The MODT RAN2/3 Report and LOWTRAN-7 Model*, PL/GPOS, Hanscom AFB, MA0173-3010, Contract F19628-91-C-0132 (1996), p. 260.
11. V.V. Osipov, N.F. Borisova, and V.V. Tsukanov, in: *Abstracts of Reports at International Radiation Symposium (IRS 2000)*, St.-Petersburg State University E30 (2000), p. 139.
12. L.S. Rothman, R.R. Gamache, R.H. Tipping, et al., J. Quant. Spectrosc. Radiat. Transfer **48**, Nos. 5–6, 469–507 (1992).
13. V.M. Osipov and N.F. Borisova, Atmos. Oceanic Opt. **11**, No. 5, 382–386 (1998).
14. M.P. Gordin, A.V. Sokolov, and G.M. Strelkov, Results of Science and Technology, VINITI, Radiotekhnika **20**, 20–289 (1980).
15. O.A. Volkovitskii, Yu.S. Sedunov, and L.P. Semenov, *High-Power Laser Radiation Propagation in Clouds* (Gidrometeoizdat, Leningrad, 1982), 312 pp.
16. V.E. Zuev, A.A. Zemlyanov, Yu.D. Kopytin, and A.V. Kuzikovskii, *High-Power Laser Radiation in the Atmospheric Aerosol* (Nauka, Novosibirsk, 1989), 224 pp.
17. V.P. Lukin, *Atmospheric Adaptive Optics* (Nauka, Novosibirsk, 1986), 248 pp.
18. V.V. Vorob'ev, *Thermal Blooming of Laser Radiation in the Atmosphere. Theory and Model Experiment* (Nauka, Moscow, 1987), 200 pp.
19. V.E. Zuev, A.A. Zemlyanov, and Yu.D. Kopytin, *Present-Day Problems of Atmospheric Optics. Nonlinear Optics of the Atmosphere* (Gidrometeoizdat, Leningrad, 1989), 256 pp.
20. V.P. Aksenov, V.A. Banakh, V.V. Valuev, V.V. Zuev, V.V. Morozov, I.N. Smalikho, and R.Sh. Tsvyk, *High-Power Laser Beams in Random-Inhomogeneous Atmosphere* (Siberian Branch of the Russian Academy of Sciences, Novosibirsk, 1998), 341 pp.
21. A.A. Averbakh, V.A. Betin, S.V. Gaponov, et al., Izv. Vyssh. Uchebn. Zaved., Ser. Radiofizika **21**, No. 8, 1077–1106 (1978).
22. I.S. Golubtsov, V.P. Kandidov, and O.G. Kosareva, Atmos. Oceanic Opt. **14**, No. 5, 303–315 (2001).
23. D.V. Vlasov, R.A. Garaev, V.V. Korobkin, and P.V. Serov, Zh. Eksp. Teor. Fiz. **76**, No. 6, 2339–2345 (1979).
24. V.V. Vorob'ev, Izv. Vyssh. Uchebn. Zaved., Ser. Radiofizika **39**, No. 8, 1014–1025 (1996).
25. G. Fibich and B. Ilan, Physica D **157**, 112–146 (2001).
26. G. Fibich and G.S. Papanicolaou, Opt. Lett. **22**, 1379–1381 (1997).
27. J.V. Moloney, M. Kolesik, M. Mlejnek, and E.M. Wright, Chaos: An Interdisciplinary Journal of Nonlinear Science **10**, No. 3, 559–569 (2000).
28. N. Akozbek, C.M. Bowden, and S.L. Chin, Laser Phys. No. 1, 77–81 (2001).
29. S.L. Chin, A. Tabelpour, J. Yang, S. Petit, V.P. Kandidov, O.G. Kosareva, and M.P. Tamarov, Appl. Phys. B. **74**, No. 1, 67–76 (2002).